Journal of Biomolecular NMR, **16:** 209–219, 2000.
KLUWER/ESCOM

Partial NMR assignments for uniformly (^{13}C, ^{15}N)-enriched BPTI in the solid state

Ann McDermott[a,*], Tatyana Polenova[a,**], Anja Bockmann[a,***], Kurt. W. Zilm[b,*], Eric K. Paulsen[b], Rachel W. Martin[b] & Gaetano T. Montelione[c]
[a]*Columbia University, Department of Chemistry, 3000 Broadway MC 3113, New York, NY 10027, U.S.A.*
[b]*Yale University, Department of Chemistry, 225 Prospect Street, New Haven, CT 06511, U.S.A.*
[c]*Rutgers University, Center for Advanced Biotechnology and Medicine, 679 Hoes Lane, Piscataway, NJ 08854-5638, U.S.A.*

Received 17 August 1999; Accepted 6 December 1999

Key words: amino acid side chain, assignment protocol, bovine pancreatic trypsin inhibitor, solid state NMR, uniform labeling

Abstract

We demonstrate that high-resolution multidimensional solid state NMR methods can be used to correlate many backbone and side chain chemical shifts for hydrated micro-crystalline U-^{13}C,^{15}N Basic Pancreatic Trypsin Inhibitor (BPTI), using a field strength of 800 MHz for protons, magic angle sample spinning rates of 20 kHz and proton decoupling field strengths of 140 kHz. Results from two homonuclear transfer methods, radio frequency driven dipolar recoupling and spin diffusion, were compared. Typical ^{13}C peak line widths are 0.5 ppm, resulting in Cα-Cβ and Cα-CO regions that exhibit many resolved peaks. Two-dimensional carbon–carbon correlation spectra of BPTI have sufficient resolution to identify and correlate many of the spin systems associated with the amino acids. As a result, we have been able to assign a large number of the spin systems in this protein. The agreement between shifts measured in the solid state and those in solution is typically very good, although some shifts near the ion binding sites differ by at least 1.5 ppm. These studies were conducted with approximately 0.2 to 0.4 μmol of enriched material; the sensitivity of this method is apparently adequate for other biological systems as well.

Introduction

Solid state NMR (SSNMR) has been a method of choice for probing structure, conformational dynamics, ionization state and hydrogen bonding for many large and insoluble biological systems. Many examples from the literature attest to the strengths of SSNMR for structural and dynamics studies; to mention just a few cases, SSNMR has provided significant insights into the structures and mechanisms of rhodopsin (Feng et al., 1997), and bacteriorhodopsin (Thompson et al., 1992), 5-enolpyruvylshikimate-3-phosphate (EPSP) synthase (McDowell et al., 1996), β-amyloid (Lansbury et al., 1995; Benzinger et al., 1998) and gramicidin (Ketchum et al., 1993). Most of the solid-state NMR experiments to date have utilized selective labeling, which tends to make these studies labor intensive and narrowly focussed. Reliable resonance assignment protocols would make SSNMR methods more powerful. Recent studies of the major coat protein of the fd bacteriophage (Marassi et al., 1997) illustrate the potential power of uniform labeling and SSNMR studies for static, oriented membrane proteins. Another appealing approach for resonance assignments of solid state proteins borrows conceptually from solution methods (Montelione and Wagner,

*To whom correspondence should be addressed. E-mail: mcdermot@chem.columbia.edu (A.M.); kurt.zilm@yale.edu (K.W.Z.).
**Present address: Hunter College, Department of Chemistry, 695 Park Avenue, New York, NY 10021, U.S.A.
***Present address: Institute de Biologie et Chemie des Proteines, UPR 412-CNRS, Laboratoire de Conformation des Proteines, 7, passage du Vercors, F-69367 Lyon Cedex 07, France.

1990; Kay et al., 1990) in that the primary tool would be multi-dimensional correlation of the isotropic backbone and side chain ^{15}N and ^{13}C resonances. The potential advantage in utilizing unoriented samples and high-resolution MAS methods is that isotropic shifts would allow for unambiguous identification of many of the side chains and therefore 'proofreading' of the assignments. Cα and Cβ isotropic shifts would also provide information on secondary structure or backbone torsion angles (Saito et al., 1983; Spera and Bax, 1991; Wishart et al., 1991; de Dios et al., 1993). The problem of site-specific backbone assignments for uniformly isotopically enriched systems has been considered (Tycko, 1996), and a recent report demonstrates that backbone assignments for some sites will be possible even at moderate field strengths (Straus et al., 1998b).

Relatively high sample spinning speeds can be utilized to establish correlations between isotropic shifts at high field strengths for biological solids. The carbon spectra of uniformly enriched proteins are sufficiently congested that spinning rates of 85–100 ppm must be used. A variety of homo- and heteronuclear transfer sequences have emerged recently (Griffin, 1998), which operate by manipulating dipolar interactions during Magic Angle Spinning (MAS). Homonuclear methods include RFDR (Bennett et al., 1992, 1998), C7 (Lee et al., 1995), POST-C7 (Hohwy et al., 1998), and CMR7 (Rienstra et al., 1998), SPC-5 (Hohwy et al., 1999), MELODRAMA (Sun et al., 1995b), DRAWS (Gregory et al., 1995), TOBSY (Baldus and Meier, 1996), USEME (Fujiwara et al., 1995) and R/L (Baldus et al., 1994). Heteronuclear methods include RFDRCP (Sun et al., 1995a), TEDOR (Hing et al., 1992), SPICP (Wu and Zilm, 1993), APHH-CP (Hediger et al., 1994, 1995; Baldus et al., 1996) and AMAP-CP (Hediger et al., 1997). The relative merits of many of these techniques have been discussed recently (Baldus et al., 1998a); they can be applied as multidimensional experiments in order to assign uniformly enriched small molecules in the solid state (Fujiwara et al., 1995; Michal and Jelinski, 1997; Hong and Griffin, 1998). Thus, the tools appear to be in place for correlation spectroscopy of proteins. Remaining obstacles concern dispersion and line widths of the systems of interest, and detection sensitivity for multidimensional experiments on sub-micromole quantities of sample.

In this report we present ^{13}C homonuclear correlation experiments for uniformly ^{13}C,^{15}N-enriched BPTI. This sample was selected because of its modest size (6.5 kDa or 58 residues) and the extensive literature about its solution NMR properties. Measurements using several field strengths B_0 are compared with the objective of assessing the dispersion and resolution in the spectra. We demonstrate that at the highest field strengths available, extensive assignments of side chain carbons can be accomplished for many amino acid side chains using 2D spectroscopy involving relatively simple recoupling pulse sequences and remarkably small amounts of isotopically enriched protein (0.2–0.4 μmol). The side chain peaks can be correlated to the backbone resonances and ultimately combined with additional measurements of tensorial properties to determine local structures and conformational dynamics in biopolymers.

Materials and methods

U-^{13}C ^{15}N BPTI was prepared by overexpression in *E. coli*, purification, refolding and re-purification as described elsewhere (Jansson et al., 1996). 5 mg of U-^{13}C, ^{15}N BPTI was mixed with 50 mg of unenriched BPTI (Cal Biochem) and crystallized by dialysis against deionized water for 1 week at room temperature in the presence of 10 μM sodium azide. The homogeneity of both the isotopically enriched and natural abundance materials was verified by mass spectrometry and SDS-PAGE gel electrophoresis. Approximately 1–2 mg of isotopically enriched material was used for spectroscopy.

300 MHz homonuclear ^{13}C spectra of microcrystalline BPTI were acquired on a Chemagnetics Infinity 300 spectrometer (Yale University) using a 3.2 mm triple resonance MAS probe (Varian-Chemagnetics, U.S.A.), a spinning speed of 11.5 kHz and sample temperature of $-10\,^{\circ}$C. The MELODRAMA $n = 2$ condition was used (spin lock field strength 23 kHz) with a mixing time of 1 ms. TPPM decoupling was applied during t_1 evolution, mixing, and acquisition with a decoupling field strength of 132 kHz. An adiabatic tangential ramped cross-polarization of 3 ms was used to transfer the proton magnetization to the carbon. 512 t_1 increments were collected with 64 scans per transient with a relaxation delay of 4 s (total aquisition time 36 h). Frequency discrimination in the indirect dimension was accomplished using the States method (States et al., 1982). The spectra were processed using FELIX (MSI) with application of a sinebell window function in both dimensions.

400 MHz homonuclear ^{13}C solid state NMR spectra were acquired on a Chemagnetics CMX400 spectrometer (Columbia) operating at Larmor frequencies of 396.5 MHz for protons, 99.7 MHz for ^{13}C, and 40.2 MHz for ^{15}N, using a 5 mm double resonance MAS probe (Chemagnetics-Otsuka Electronics, U.S.A.), spinning speed 8.2 kHz, and a sample temperature of $-10\,^{\circ}C$. The $n = 2$ condition MELODRAMA sequence was used (spin lock field strength 16.5 kHz) with a mixing time of 1 ms. TPPM decoupling (Bennett et al., 1995) (field strength 80 kHz) was applied during t_1 evolution, mixing and acquisition. An adiabatic linear ramped cross polarization of 3 ms was used to transfer the proton magnetization to the carbon. 179 t_1 increments were collected with 256 scans per increment, and a relaxation delay of 3 s (total acquisition time of 38 h). TPPI (Marion and Wüthrich, 1983) was used for phase sensitive detection in the indirect dimension. The spectra were processed in FELIX (MSI). Shifted (90°) sinebell window functions were applied in both dimensions.

800 MHz homonuclear ^{13}C spectra of microcrystalline BPTI were acquired using a Varian INOVA 800 MHz spectrometer (Yale University) outfitted with a double resonance probe with 2.5 mm rotors, ca 20 kHz sample spinning speed (see specific details below), 140 kHz proton decoupling (TPPM), and a sample temperature of $10\,^{\circ}C$ was maintained during the experiment. Two spectra utilizing the RFDR sequence are presented. In one (Figure 1c), carbon detection windows were 80 kHz in both dimensions, the initial carbon excitation was accomplished with a 3 ms cross-polarization (square pulse); 1000 scans per t_1 increment, and 160 t_1 increments were used with a recycle delay of 1.5 s to give a 66 h experiment. The spinning speed was 20.08 kHz and six cycles of XY-8 phase cycled π pulses were used to give a 2.4 ms mixing time. In the other (Figure 2a), spectral windows of 80 kHz and 32.494 kHz were used for the direct and indirect dimensions, respectively, and the carbon magnetization was excited using cross-polarization for 80 μs (square pulse); 576 scans were collected for each time increment, and 160 t_1 increments were collected with a pulse delay of 1.5 s, to give a 38 h experiment. The spinning speed was 19.23 kHz and four cycles of XY-8 phase cycled π pulses were used to give a total mixing time of 1.66 ms. One experiment utilizing proton assisted spin diffusion is presented (Figure 2b). Spectral windows of 80 and 32.494 kHz were used. 256 scans per t_1 increment and 131 t_1 increments were collected with a pulse delay of 1.5 s to give a 14 h experiment. The spinning speed was 19.6 kHz and the mixing time (without decoupling) was 50 ms. TPPI (Marion and Wüthrich, 1983) was used for phase sensitive detection in the indirect dimension. Data were processed using FELIX (MSI). Shifted (90°) sinebell window functions were applied in both dimensions, except as noted.

Results and discussion

Carbon–carbon correlation spectra of uniformly enriched BPTI collected at 300, 400, and 800 MHz are compared in Figure 1. Two-dimensional carbon–carbon correlation spectra for roughly 0.2 μmol of micro-crystalline U-^{13}C,^{15}N BPTI are shown, for which the mixing period consisted of MELODRAMA (for 300 and 400 MHz spectra), and RFDR (for 800 MHz spectra). The sample spinning speed of 19.8 kHz in the 800 MHz spectra was selected so as to avoid rotational resonance conditions between the carbonyl carbons and any of the aliphatic carbons. Sample temperatures were maintained between $-10\,^{\circ}C$ (300 and 400 MHz spectra) and $5\,^{\circ}C$ (800 MHz spectra) throughout. Most of the experimental settings were similar for the three data sets (cross-polarization contact time, mixing time during the MELODRAMA or RFDR transfers, total acquisition time). The sensitivity in the 800 MHz spectra is dramatically enhanced above those collected at 300 MHz or 400 MHz. In the 300 MHz spectra higher decoupling power results in better recoupling of the resonances as compared with the 400 MHz spectra, but the sensitivity is significantly lower than in the 400 MHz data. The decoupling strength does have the expected effect upon the line widths as assessed from the diagonal peaks. In order to apply higher decoupling strengths, small stators were used, so that only a fraction of the sample could be packed into the rotors (ca. 0.25) and thus the net gain in sensitivity due to the improved decoupling was compromised. In addition, the higher spinning speeds made dehydration of the sample a significant concern; rubber gaskets were included in the rotor assembly to minimize this problem.

The proton T_1 value was estimated from inversion recovery experiments at 800 MHz. Relaxation data were acquired using both direct detection of the protons, and indirect detection via CP to ^{13}C, and seven time points were acquired. The relaxation curves were apparently single exponential, and a proton T_1 of 0.4 s was determined by least squares fitting of the data. The

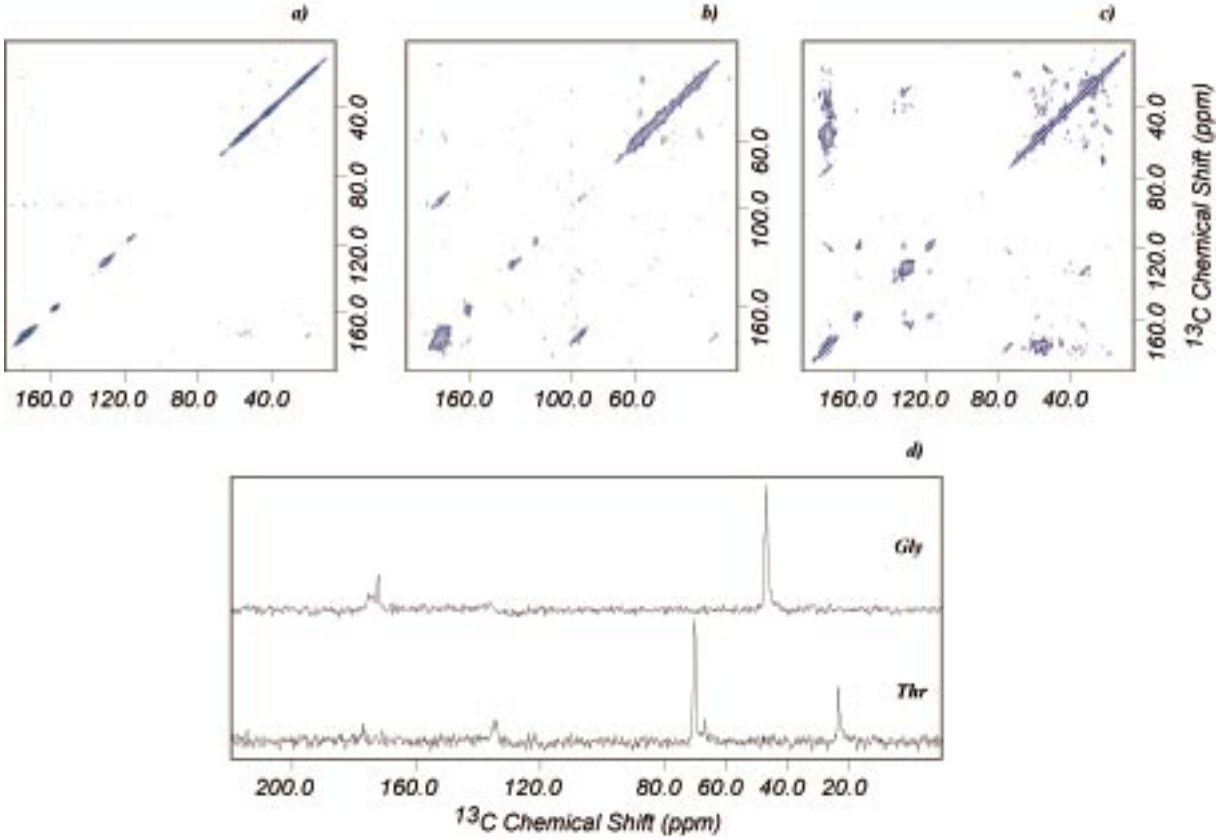

Figure 1. Two-dimensional carbon-carbon correlation spectra for microcrystalline U-^{13}C,^{15}N-BPTI at 300, 400, and 800 MHz are compared. (a) Spectrum at 300 MHz (spinning speed 11.5 kHz, sample temperature −10 °C). Carbon recoupling was established using the n = 2 condition of the MELODRAMA mixing sequence (spin-lock field of 23 kHz) with a 1 ms mixing time. Proton decoupling field was 135 kHz. Total acquisition time was 36 h. (b) Spectrum at 400 MHz (spinning speed 8.2 kHz, sample temperature −10 °C). Carbon recoupling was established using the n = 2 condition of the MELODRAMA mixing sequence (spin-lock field of 16.5 kHz) with a 1 ms mixing time. Proton decoupling field was 80 kHz. Total acquisition time was 38 h. (c) Spectrum at 800 MHz (spinning speed 19.8 kHz, sample temperature 5 °C). Carbon recoupling was established using the RFDR mixing sequence with a 1.6 ms mixing time. Proton decoupling field was 140 kHz. Total acquisition time was 38 h. Panel (d) shows representative slices of the C-C 2D taken at 800 MHz, illustrating the intensities and signal-to-noise ratios of the important cross peaks.

observed proton T_1 is sufficiently short to accommodate a recycle delay of only 1.5 s, largely mandated to minimize probe heating effects.

Many prominent cross peaks corresponding to directly bonded pairs can be seen in the 800 MHz spectrum, including the CO-Cα region, numerous Cα-Cβ cross peaks, and intra-aromatic cross peaks. The line widths of the cross peaks appear to be approximately 0.5 ppm throughout the spectrum, and may be in large part determined by the J-couplings (35 Hz for the homonuclear Cα-Cβ coupling; 55 Hz for the homonuclear Cα-CO coupling, and 15 Hz for the heteronuclear N-C coupling) (Clore and Gronenborn, 1994). In contrast, few cross peaks of interest could be detected at lower field strengths.

In Figure 2 we contrast the aliphatic or 'Cα-Cβ' regions for a spectrum in which the RFDR pulse sequence was used to achieve transfer of Zeeman order to one for which simple proton assisted spin diffusion (delay with longitudinal carbon magnetization and no RF proton decoupling) was used to establish transfer. The intensities of the cross peaks differ substantially for the RFDR and the spin diffusion sequences, where typically pairs of peaks characterized by large differences in chemical shift give rise to more prominent cross peaks if the transfer is driven by the RFDR pulse sequence, and those with small differences in chemical shift are more prominent if spin diffusion is used. Assignment of many side chains is possible on the basis of the spectra presented in Figure 2. In Figure 3 the

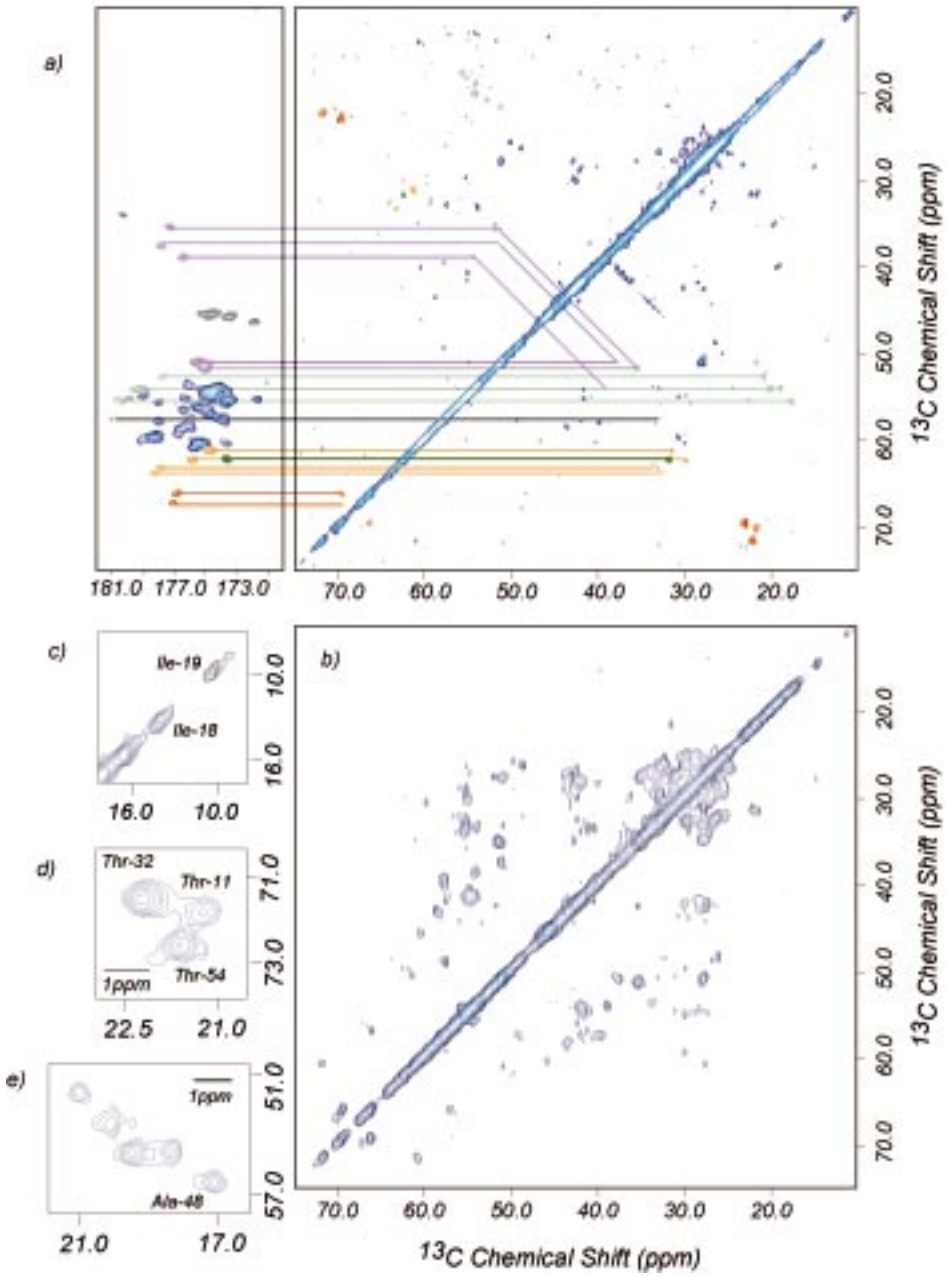

Figure 2. Two-dimensional carbon–carbon correlation spectra for micro-crystalline U-^{13}C,^{15}N BPTI. A short cross-polarization period (50 μs) achieved selective polarization transfer to protonated carbons in both cases. Spectra were processed in FELIX (MSI); a 90° sine-bell window function in both dimensions was applied. Two mixing sequences are contrasted: (a) RFDR (1.6 ms resulting from four cycles of the XY-8 mixing sequence). The data were collected in 72 h, involving 160 increments and 512 scans per increment, with a pulse delay of 1.5 s. In the RFDR spectrum, the CO-Cα region and the aliphatic region are shown on the same scale. The assigned cross peaks are color coded according to the amino acid type. The horizontal lines are drawn to demonstrate the walks through CO-Cα–Cβ resonances. For the three Asn residues, a CO-Cα–Cβ-Cγ walk is shown. For the site-specific assignments of the aliphatic cross peaks, refer to Figure 3. The sequence-specific assignments of the CO-Cα resonances are given in Figure 4. The Met and Gly cross peaks were identified solely on comparison with solution NMR data; for all others the identification is based on reading through the side-chain spin system. The two Leu residues (6 and 29) can also be identified in the aliphatic region, and the aromatic–aliphatic and aromatic–aromatic cross peaks for Tyr and Phe can be identified, but in these cases ambiguities occur in the correlations, so these were not highlighted. Expansions (c), (d) and (e) come from spectrum 2(a) and illustrate the peak shapes for Ile, Thr, and Ala residues, respectively. (b) Proton assisted spin diffusion (50 ms longitudinal mixing without proton decoupling). In the spin diffusion spectrum, the aliphatic region is displayed to emphasize Cα-Cβ cross peaks. The intensities of the cross peaks differ substantially for the RFDR and the spin diffusion sequences, where typically those with large differences in chemical shift are more prominent in the RFDR data and those with small differences in chemical shift are more prominent in the spin diffusion data set.

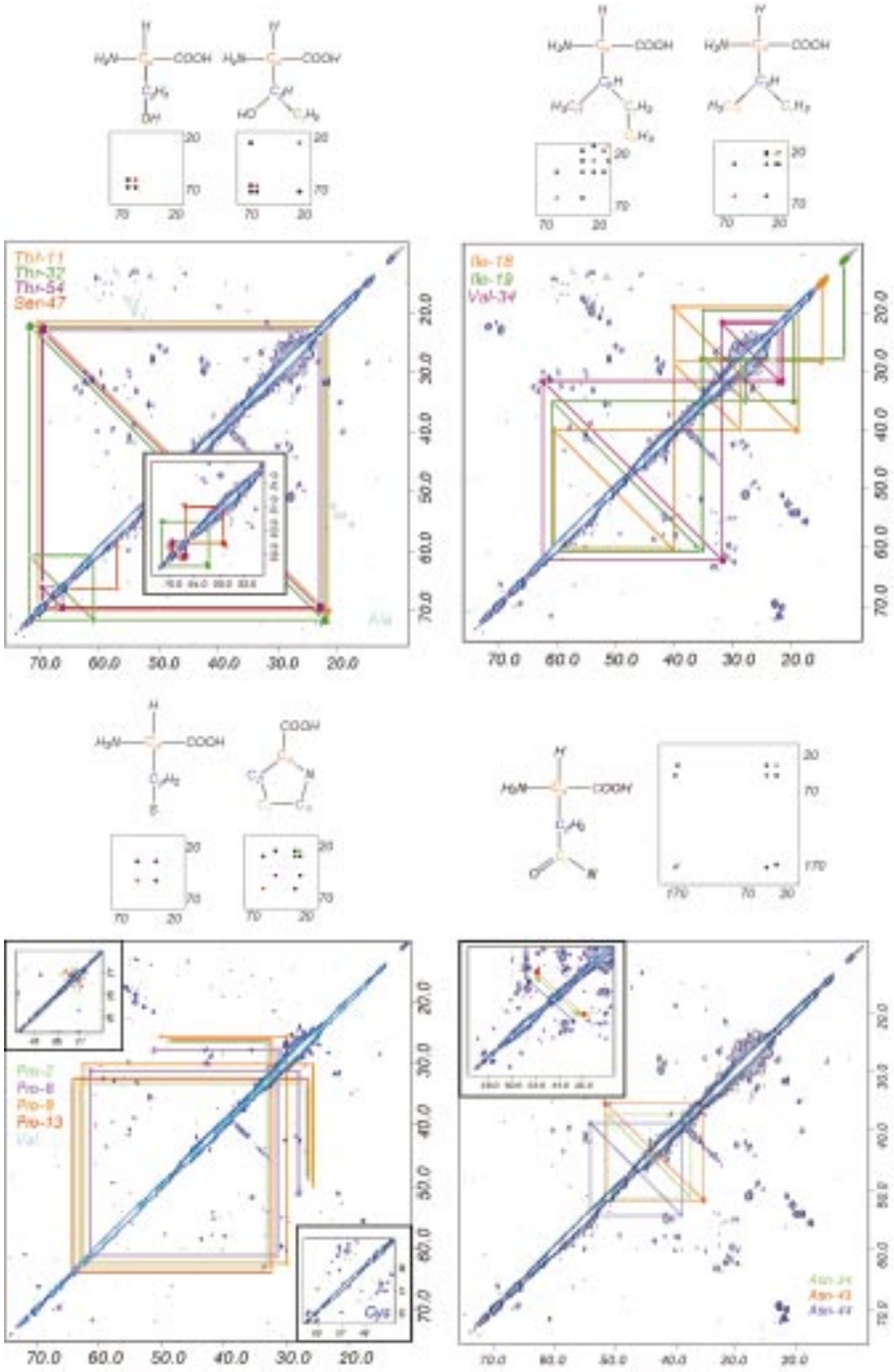

Figure 3. Side-chain correlations are illustrated for: Top left: the three Thr and the unique Ser (RFDR data set as described in Figure 2 with spin diffusion inset); top right: the unique Val and both Ile (RFDR data set as described in Figure 2, another RFDR data set inset); bottom left: all four Pro (RFDR data set as described in Figure 2 with spin diffusion inset); bottom right: all three Asn (RFDR data set as described in Figure 2 with spin diffusion inset). Walks through the side chains are illustrated with horizontal and vertical bars connecting related cross peaks in the sequence. The data are identical to those shown in Figure 2, except that for the Pro and Asn figures resolution enhancement was used in processing (shifted sine-bell with a 60° phase). Insets illustrate that the same cross peaks can be found in the data set for which spin diffusion was used to facilitate mixing, often with stronger intensity (except for the top right panel for Ile and Val, where the inset is another RFDR data set). The assignments rely heavily on the RFDR data set, but the spin diffusion spectrum (Figure 2) was also important, primarily for confirming the methylene–methylene cross peaks of Pro and the methylene–methyne cross peaks of Cys, Asn and Thr. Five well-resolved cross peaks in the region corresponding to shifts of 17–21 ppm and 51–55 ppm are assignable as Ala (Figure 3a), and six cross peaks in the region corresponding to shifts of 42–46 ppm and 54–61 ppm are assignable as Cys (inset at lower left).

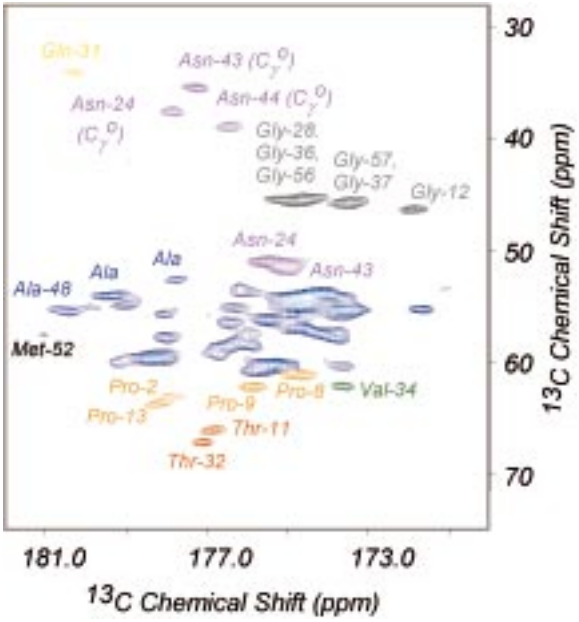

Figure 4. Backbone (CO-Cα region) correlations, including assigned Thr, Asn, Pro, Val, Gly, Gln, Met, and Ala residues. Data collection as described in the caption for Figure 2. The spectrum was processed in FELIX (MSI). A 60° sine-bell window function was applied in both dimensions to enhance resolution.

same spectra from Figure 2 are presented with horizontal and vertical bars to guide the eye through the recognition of the spin systems present in BPTI. Many amino acid side-chain resonances can be identified and correlated to those of the protein backbone. For some amino acids, unambiguous topologies can be established from these 2D spectra. We list a comparison of the expected and experimentally observed numbers of that type of amino acid: Thr (3/3), Ser (1/1), Val (1/1), Ile (2/2), Pro (4/4), Asn (3/3), Gln (1/1). Other amino acids give rise to cross peaks as expected but cannot be site-specifically assigned: Ala (5/6), Gly (5/5, not all resolved), Cys (6/6), Phe (4/4 unassigned), Tyr (4/4), Leu (2). The following residues are apparently weak due to structural heterogeneity: Asp, Glu, Lys, Arg. Finally, the following amino acids are not present in BPTI: His, Trp.

Many of the peaks in the CO-Cα region can also be resolved and assigned, as illustrated in Figure 4. When resolution enhancement (a shifted sine-bell with a 60° shift) was used to process the data, many of the peaks could be identified through comparison between cross peaks in the Cα-Cβ and the CO-Cα regions. Figure 4 illustrates these assignments. Two bond transfers can be seen in this region as well, particularly so for the spin diffusion data set. For example, both the Thr and the Ala residues show well resolved Cβ-CO cross peaks, which are useful for identifying the CO resonances for these amino acids.

It is of interest to compare the carbon shift values as measured in the solid state to those measured in solution state. Cole and Torchia (1991) previously observed that isotropic shifts tend to be similar in the solid and the solution state in connection with extensive comparative data on staphylococcal nuclease. Many aspects of the sample conditions necessarily differ for solution vs. solid state measurements (pH, ionic strength) but it is known that with the important exception of the easily ionized residues, many of the carbon shifts for BPTI are rather immune to these issues in solution state (Tuchsen and Hansen, 1988). Table 1 indicates the comparison between isotropic chemical shifts measured in solution and in the solid state. In making the comparison of carbon shifts measured in the solid state vs. in solution we have utilized proposed *sequence-specific* assignments for our SSNMR data. While the spin systems are unambiguously identified through correlations in isotropic shifts, as illustrated in Figure 3, sequence-specific assignments would normally be determined by identifying sequential backbone connectivities, which we have not completed yet. Sequence-specific assignments can be unambiguously determined for the amino acids in which the sequence provides only one example of a particular amino acid (Ser, Val, Gln). We propose that some other sequence-specific assignments can be determined by comparisons between solution and the solid state values; the sharp agreement in certain side-chain shift patterns (see, for example Thr or Ile) indicates that assignments based upon solution NMR chemical shift values are correct and the similarity of the isotropic shifts between solution and solid state is not fortuitous. Comparison of values for the more trivial spin systems (Gly, Ala, Cys) is probably not as meaningful. Measurements in solution state were performed as part of our parallel efforts to develop general methods for automated analysis of multidimensional NMR spectra of proteins. These solution-state ^{13}C assignments are also reported in Table 1. The solution chemical shifts are referenced relative to DSS and differ in some respects from previously reported values, presumably because of differences in referencing (Wagner and Bruhwiler, 1986; Tuchsen and Hansen, 1988). The solid state NMR spectra were referenced assuming that the most deshielded carbon is attributed to the delta position of Ile 19 and is at

Table 1. Isotropic chemical shifts for carbon resonances in BPTI

Amino acid	Cα:Soln (SS), ppm	Cβ:Soln (SS), ppm	Cγ1:Soln (SS), ppm	Cγ2′:Soln (SS), ppm	Cδ:Soln (SS), ppm	CO:Soln (SS), ppm
Asn-24	50.8 (50.9)	38.5 (37.6)	(177.7)			175.5 (175.2)
Asn-43	51.1 (51.6)	35.7 (35.4)	(177.0)			174.9 (174.8)
Asn-44	54.1 (54.4)	39.6 (38.9)	(176.3)			174.4
Ile-18	60.4 (60.2)	40.1 (39.9)	18.9 (19.2)	**27.4 (28.5)**	14.3 (14.9)	175.8
Ile-19	**61.3 (60.2)**	35.9 (34.9)	**17.6 (19.5)**	27.7 (27.9)	10.9 (10.9)	176.7
Ser-47	56.4 (56.8)	**67.9 (66.1)**				173.7
Thr-11	67.3 (67.2)	70.5 (70.1)	22.0 (21.6)			177.0 (177.1)
Thr-32	60.8 (60.9)	71.2 (71.6)	22.5 (22.2)			175.6 (175.6)
Thr-5	66.4 (66.2)	69.5 (69.5)	22.8 (22.8)			176.6 (176.8)
Val-34	62.6 (62.3)	31.3 (31.8)	22.5 (22.1)	(21.6)		174.5 (174.0)

In each case the connectivities within the ^{13}C SSNMR data were established through the two 2D spectra shown and were sufficient to the amino acid type corresponding to the resonances. Site-specific assignments for Val 43 and Ser 47 are possible since they are the only Val and Ser in BPTI; those for the Thr, Ile, and Asn are proposed based only upon comparison of the pattern of solution and solid state isotropic shifts. Rms deviations between solution and solid state shifts are approximately 0.5 ppm. Shifts that differ by more than 1.0 ppm are indicated in bold and appear in a cluster on the surface of the protein on the side of the molecule that is more electrostatically charged (Figure 5). When more assigned sites were included (ones which were somewhat less secure because there are more of that residue type, such as Ala, Pro and Cys, see Supplementary material), the pattern persists that the perturbed sites are all on one surface-exposed cluster, presumably because of solid state contacts.

10.9 ppm relative to DSS. In total we were able to correlate more than half the side chains using only these two 2D spectra, although sequence-specific assignments are unambiguous for only about a quarter of the residues. The solution and solid state shifts agree within 1 ppm except for a few residues (Ile18, Ile19, Ser47) that are near the ion binding site and the ligands Lys46 and Arg20 for the ion (Figure 5). Since our sample was dialyzed and recrystallized from distilled water it is likely that the ion binding site is unoccupied and therefore the nearby residues are structurally perturbed.

These experiments offer optimism relative to many of the typical problems encountered in SSNMR and relative to the future of resonance assignment of uniformly isotopically enriched biopolymers. One issue relates to decoupling protons from the carbon nuclei during detection; decoupling methylenes is a notorious problem for solid state NMR measurements on organic solids. The Pro residues contain strongly coupled proton spin systems with several flanking methylene units; these residues exhibit very strong signals in our data. In this regard the high spinning speeds and decoupling strengths used in the present study are probably crucial. It will be of interest to study selectively deuterated proteins, and assess these spectra as a function of proton decoupling fields. The effects of the homonuclear couplings in determining the line widths of the carbon resonances are presumably substantial, particularly the J couplings. In addition, the residual broadening due to incomplete MAS averaging of the ^{13}C-^{13}C dipolar couplings for spin systems that have congested isotropic shifts may still be important. In this respect, constant-time experiments may be of interest (Straus et al., 1996, 1998a).

Groups in intermediate exchange typically show depressed SSNMR intensities over very broad temperature ranges due to the many time-scales on which conformational dynamics might interfere with coherent evolution processes (Long et al., 1994). BPTI has many amino acids that are known to be in or near intermediate exchange in solution near our experimental temperature (Wagner et al., 1976). Phe22, Phe45, Tyr23 and Tyr35 rings are probably in slow exchange (<1 s^{-1}) (Wagner, 1983); Cys14 and 38 undergo an isomerization in intermediate exchange ($\sim$10 s^{-1}) (Otting et al., 1993) and other aromatic rings (including those that are solvent exposed): Phe4 and 33 and Tyr10 and 21, probably undergo faster flipping ($>10^5$ s^{-1}) (Wagner, 1983). It remains of interest to study the signal strengths as a function of sample temperature; at present we have insufficient data to relate

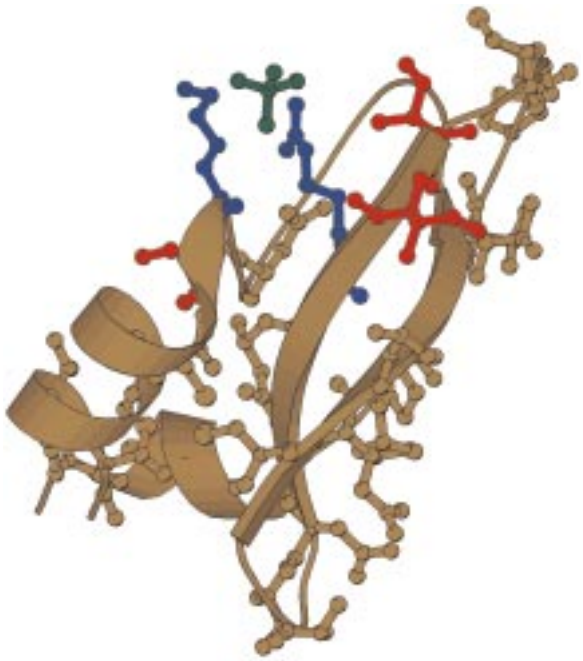

Figure 5. Cartoon of BPTI based on the Protein Data Bank file (6pti). Side chains indicated in molecular detail were assigned. Red side chains exhibited carbon chemical shift deviations (solid state vs. solution) outside the typical range associated with the experimental error (i.e. more than 2 σ or more than 1 ppm, Ile 18, Ile 19 and Ser 47). Brown side chains had shifts that were within experimental error; these residues are distributed throughout the molecule. Two residues, Arg 46 and Lys 20, serve as ligands for the ion binding site and are rendered in blue. The perturbed side chains appear in a patch near these charged side chains and the ion binding pocket. Graphical representation prepared using MolScript (Kraulis, 1991).

dynamics to peak intensity in a reliable way. However, from a cursory glance it is clear that the Cys residues in intermediate exchange exhibit depressed intensities relative to the other Cys residues, and that aromatic rings in the rigid limit exhibit strong assignable resonances while the other ring carbons appear to be broader.

An unanticipated 'blind spot' in our measurements concerns ionization phenomena. Many amino acids with charged side chains (e.g. Glu, Asp, Arg, Lys) exhibit resonances that are systematically weak in intensity, or broad and unresolved, as if their structures are heterogeneous under the low ionic strength crystallization conditions. Some of these residues are also known to exhibit strongly pH dependent shifts (Tuchsen and Hansen, 1988).

Since these experiments have been performed on a fraction of a micromole of protein, the prospects are excellent in terms of studies of domains in the context of large complexes. The available volume in a high speed rotor has been only partially utilized (<10%) and so complexes with large effective molecular weights, with uniformly isotopically enriched domains of the size of BPTI, can probably be studied with multidimensional methods. A number of straightforward experiments can be proposed on the basis of this pilot study. The good agreement between solution and solid state shifts indicates that assignments might be 'borrowed' from solution NMR as a starting hypothesis for SSNMR assignments. Furthermore, these measurements could be used for studying binding faces in macromolecular assemblies via chemical shift perturbations.

Our optimistic outlook based on these spectra differs somewhat from the conclusions offered in previous discussions of backbone resonances and the prospects for complete assignment by SSNMR methods (Tycko, 1996). The use of resolved side-chain resonances and the unambiguous information of amino acid identity simplifies the assignment protocol significantly and provides opportunities for 'proofreading' the assignments. Even if the backbone resonances prove to be relatively poorly resolved, these side-chain resonances will be important in the protocol for partial assignments. The dispersion and line widths for BPTI are relatively favorable; of course it is not yet clear whether other systems of biological interest will exhibit this resolution.

The effort to assign NMR spectra of proteins in the solid state has many remaining spectroscopic objectives. Heteronuclear C-N correlation spectra at high fields represent a very important objective. These spectra have the potential to be more resolved than the homonuclear spectra, and provide opportunities for efficient, directed one bond transfers through the backbone (Baldus et al., 1998b). It remains to be seen how the resolution of the backbone ^{15}N resonances at high fields will compare with those observed for ^{13}C in this work. Our observation that the ^{13}C resonances associated with ionic residues are significantly broader, presumably due to structural heterogeneity linked to crystallization conditions, would suggest that sample preparation protocols will be as important, if not more so, than careful spectroscopic practice in obtaining the ultimate achievable resolution in such experiments. Assuming that such potential difficulties can be generally addressed, it is our hope that these methods will be combined with semi-selective isotopic labeling schemes (Rosen et al., 1996; Hong, 1999) and block labeling schemes (Xu et al., 1999) to achieve use-

ful partial assignments for side chain and backbone, that will serve as the basis for structural and dynamic studies of proteins.

Conclusions

High field spectra of uniformly isotopically enriched solid state BPTI can be partially assigned using relatively simple 2D methods and modest amounts of isotopically enriched protein. In particular, the side chains of approximately half of the 58 residues were correlated back to the α resonance and in many cases to the carbonyl, using only a pair of simple 2D correlation experiments. Based upon unique amino acids and on comparison with solution NMR data, side chains (roughly a quarter of all residues) could be unambiguously identified. Improved performance at 800 MHz as compared with lower field strengths is dominated by the fact that the sensitivity is dramatically better, but the effective resolution in these simple homonuclear correlation experiments might also be improved significantly due to a contribution for C-C J couplings that are fixed over the field range. Presumably physical homogeneity of the samples is also important, and will in part guide the selection of future systems, although this point remains to be examined systematically. We propose that these methods might allow for nearly complete resonance assignments in low molecular weight biological solids in the near future.

Acknowledgements

The authors recognize the generous support of the Wm. M. Keck Foundation for the 800 MHz instrumentation at Yale University. This work was partially supported by the Charles Goodyear Cooperative Research and Development Grant number 96G032 from Connecticut Innovations, Inc. and by NIH grants GM58171 and 49964.

References

Baldus, M., Geurts, D.G., Hediger, S. and Meier, B.H. (1996) *J. Magn. Reson.*, **A118**, 140–144.

Baldus, M. and Meier, B.H. (1996) *J. Magn. Reson.*, **A121**, 65–69.

Baldus, M., Geurts, D.G. and Meier, B.H. (1998a) *SSNMR*, **11**, 157–168.

Baldus, M., Petkova, A.T., Herzfeld, J. and Griffin, R.G. (1998b) *Mol. Phys.*, **95**, 1197–1207.

Baldus, M., Tomaselli, M., Meier, B.H. and Ernst, R.R. (1994) *Chem. Phys. Lett.*, **230**, 329–336.

Bennett, A.E., Ok, J.H., Griffin, R.G. and Vega, S. (1992) *J. Chem. Phys.*, **96**, 8624–8627.

Bennett, A.E., Rienstra, C.M., Auger, M., Lakshmi, K.V. and Griffin, R.G. (1995) *J. Chem. Phys.*, **103**, 6951–6958.

Bennett, A.E., Rienstra, C.M., Griffiths, J.M., Zhen, W.G., Lansbury, P.T. and Griffin, R.G. (1998) *J. Chem. Phys.*, **108**, 9463–9479.

Benzinger, T.L.S., Gregory, D.M., Burkoth, T.S., Miller-Auer, H., Lynn, D.G., Botto, R.E. and Meredith, S.C. (1998) *Proc. Natl. Acad. Sci. USA*, **95**, 13407–13412.

Clore, G.M. and Gronenborn, A.M. (1994) *Methods Enzymol.*, **239**, 349–363.

Cole, H.B.R. and Torchia, D.A. (1991) *Chem. Phys.*, **158**, 278–281.

de Dios, A.C., Pearson, J.G. and Oldfield, E. (1993) *Science*, **260**, 1491–1495.

Feng, X., Verdegem, P.J.E., Lee, Y.K., Sandström, D., Edén, M., Bovee-Geurts, P., de Grip, W.J., Lugtenburg, J., de Groot, H.J.M. and Levitt, M.H. (1997) *J. Am. Chem. Soc.*, **119**, 6853–6857.

Fujiwara, T., Sugase, K., Kainosho, M., Ono, A., Ono, A.M. and Akutsu, H. (1995) *J. Am. Chem. Soc.*, **117**, 11351–11352.

Gregory, D.M., Mitchell, D.J., Stringer, J.A., Kiihne, S., Shiels, J.C., Callahan, J., Mehta, M.A. and Drobny, G.P. (1995) *Chem. Phys. Lett.*, **246**, 654–663.

Griffin, R.G. (1998) *Nat. Struct. Biol.*, **5**, 508–512S.

Hediger, S., Meier, B.H. and Ernst, R.R. (1995) *Chem. Phys. Lett.*, **240**, 449–456.

Hediger, S., Meier, B.H., Kurur, N.D., Bodenhausen, G. and Ernst, R.R. (1994) *Chem. Phys. Lett.*, **223**, 283–288.

Hediger, S., Signer, P., Tomaselli, M., Ernst, R.R. and Meier, B.H. (1997) *J. Magn. Reson.*, **125**, 291–301.

Hing, A.W., Vega, S. and Schaefer, J. (1992) *J. Magn. Reson.*, **96**, 205–209.

Hohwy, M., Jakobsen, H.J., Eden, M., Levitt, M.H. and Nielsen, N.C. (1998) *J. Chem. Phys.*, **108**, 2686–2694.

Hohwy, M., Rienstra, C.M., Jaroniec, C.P. and Griffin, R.G. (1999) *J. Chem. Phys.*, **110**, 7983–7992.

Hong, M., 1999 ENC Conference Abstract, Orlando, FL, M&T Poster #73.

Hong, M. and Griffin, R.G. (1998) *J. Am. Chem. Soc.*, **120**, 7113–7114.

Jansson, M., Li, Y.C., Jendeberg, L., Anderson, S., Montelione, G.L. and Nilsson, B. (1996) *J. Biomol. NMR*, **7**, 131–141.

Kay, L.E., Ikura, M., Tschudin, R. and Bax, A. (1990) *J. Magn. Reson.*, **89**, 496–514.

Ketchum, R.R., Hu, W. and Cross, T.A. (1993) *Science*, **261**, 1457–1460.

Lansbury Jr., P.T., Costa, P.R., Griffiths, J.M., Simon, E.J., Auger, M., Halverson, K.J., Kocisko, D.A., Hendsch, Z.S., Ashburn, T.T., Spencer, R.G.S., Tidor, B. and Griffin, R.G. (1995) *Nat. Struct. Biol.*, **2**, 990–998.

Lee, Y.K., Kurur, N.D., Helmle, M., Johannessen, O.G., Nielsen, N.C. and Levitt, M.H. (1995) *Chem. Phys. Lett.*, **242**, 304–309.

Long, J.R., Sun, B.Q., Bowen, A. and Griffin, R.G. (1994) *J. Am. Chem. Soc.*, **116**, 11950–11956.

Marassi, F.M., Ramamoorthy, A. and Opella, S.J. (1997) *Proc. Natl. Acad. Sci. USA*, **94**, 8551–8556.

Marion, D. and Wüthrich, K. (1983) *Biochem. Biophys. Res. Commun.*, **113**, 967–974.

McDowell, L.M., Klug, C.A., Beusen, D.D. and Schaefer, J. (1996) *Biochemistry*, **35**, 5395–5403.

Michal, C.A. and Jelinski, L.W. (1997) *J. Am. Chem. Soc.*, **119**, 9059–9060.

Montelione, G.T. and Wagner, G. (1990) *J. Magn. Reson.*, **87**, 183–188.
Otting, G., Liepinsh, E. and Wüthrich, K. (1993) *Biochemistry*, **32**, 3571–3582.
Rienstra, C.M., Hatcher, M.E., Mueller, L.J., Sun, B.-Q., Fesik, S.W., Herzfeld, J. and Griffin, R.G. (1998) *J. Am. Chem. Soc.*, **120**, 10602–10612.
Rosen, M.K., Gardner, K.H., Willis, R.C., Parris, W.E., Pawson, T. and Kay, L.E. (1996) *J. Mol. Biol.*, **263**, 627–636.
Saito, H., Tabeta, R., Shoji, A., Ozaki, T. and Ando, I. (1983) *Macromolecules*, **16**, 1050–1057.
Spera, S. and Bax, A. (1991) *J. Am. Chem. Soc.*, **113**, 5490–5492.
States, D.J., Haberkorn, R.A. and Ruben, D.J. (1982) *J. Magn. Reson.*, **48**, 286–292.
Straus, S.K., Bremi, T. and Ernst, R.R. (1996) *Chem. Phys. Lett.*, **262**, 709–715.
Straus, S.K., Bremi, T. and Ernst, R.R. (1998b) *J. Biomol. NMR*, **12**, 39–50.
Sun, B.Q., Costa, P.R. and Griffin, R.G. (1995a) *J. Magn. Reson.*, **A112**, 191–198.
Sun, B.Q., Costa, P.R., Kocisko, D., Lansbury, P.T. and Griffin, R.G. (1995b) *J. Chem. Phys.*, **102**, 702–707.
Thompson, L.K., McDermott, A.E., Raap, J., van der Wielen, C.M., Lugtenberg, J., Herzfeld, J. and Griffin, R.G. (1992) *Biochemistry*, **31**, 7931–7938.
Tuchsen, E. and Hansen, P.E. (1988) *Biochemistry*, **27**, 8568–8576.
Tycko, R. (1996) *J. Biomol. NMR*, **8**, 239–251.
Wagner, G. (1983) *Quart. Rev. Biophys.*, **16**, 1–57.
Wagner, G. and Bruhwiler, D. (1986) *Biochemistry*, **25**, 5839–5843.
Wagner, G., DeMarco, A. and Wüthrich, K. (1976) *Biophys. Struct. Mech.*, **2**, 139–158.
Wishart, D.S., Sykes, B.D. and Richards, F.M. (1991) *J. Mol. Biol.*, **222**, 311–333.
Wu, X. and Zilm, K.W. (1993) *J. Magn. Reson.*, **A104**, 154–165.
Xu, R., Ayers, B., Cowburn, D. and Muir, T. (1999) *Proc. Natl. Acad. Sci. USA*, **96**, 388–393.